The effect of oxygenated species on the fuel-rich oxidation of CH_4 in the context of polygeneration: Extinction, CO-concentration and temperature measurements

D. Nativel, J. Herzler, M. Fikri, C. Schulz
Institute for Combustion and Gas Dynamics – Reactive Fluids
University of Duisburg-Essen,
Duisburg, Germany

1 Introduction

Polygeneration in internal combustion engines enables a variable generation of mechanical power and valuable chemicals based on reactions under fuel-rich conditions depending on the fuel/air equivalence ratio ϕ [1]. This may help to mitigate one of the main challenges of future energy systems – accommodating fluctuations in electricity supply and demand. Investments in devices for grid stabilization could be more economical if they have a second use [1]. In this context, the IC engine is typically operated in homogeneous-charge compression-ignition (HCCI) mode to overcome the limitations of spark ignition due to the low flame speeds at fuel-rich conditions. To decrease the intake temperature required to initiate reactions in the available time scale, additives like n-heptane have been used to increase the reactivity of methane [2]. The maximum mechanical power is generated at stoichiometric conditions and at ϕ = 2, syngas (carbon monoxide and hydrogen) and less mechanical power is generated. At even more fuel-rich conditions, besides syngas also higher hydrocarbons are produced. At ϕ = 10, about 50 % syngas and 50 % higher hydrocarbons are formed from methane and methane/additive mixtures [2]. Under such fuel-rich conditions, the reaction-induced temperature increase is low enough that the final temperature stays below the lower limit of soot formation. The disadvantage is, however, the relatively low conversion of methane at the related temperatures. To increase the conversion of the fuel by choosing less fuel-rich conditions while avoiding soot formation, oxygenated additives (e.g., diethyl ether, DEE or methanol) are of interest. Indeed, they shift the onset temperature for soot formation to higher temperatures.

The influence of oxygenated components such as alcohols or ethers on soot formation has been investigated before in shock tubes [3], engines [4], and flames [5]. These studies showed that the presence of oxygenated components can significantly reduce the soot yield. In the study of Hong et al.

Correspondence to: damien.nativel@uni-due.de

[3], it is also shown that the so-called soot "bell-shaped" curve (i.e., the temperature window where soot forms) shifts to higher temperatures in the presence of oxygenated components. Tunable diode laser absorption spectroscopy (TDLAS) is a sensitive, non-intrusive and highly selective method that can be used to detect species and measure temperature in harsh environments with high time resolution [6]. TDLAS was used in our previous work for time-resolved measurements of temperature and CO concentration in a shock tube [7, 8]. This paper aims at studying the oxidation of fuel-rich CH_4, CH_4/DEE and CH_4/CH_3OH mixtures to investigate the soot behavior that limits the polygeneration process to very fuel mixtures. Simultaneous measurements of laser extinction at 633 nm and CO concentration and temperature using TDLAS were performed and the results were compared with chemical-kinetics based simulations [9-11].

2 Experimental details

Laser extinction, time-resolved temperature, and CO concentration profiles were measured in a shock tube behind reflected shock waves at ~5 bar in the temperature range of 1484–1875 K. The length of the driver and driven sections and the inner diameter of the shock tube are 3.6, 7.3, and 0.08 m, respectively [12, 13]. The driven section is equipped with four pressure transducers (PCB model 112A03) from which the shock velocity is obtained, which was used to calculate temperature and pressure behind the reflected shock wave using ideal shock relations (with a temperature and pressure uncertainty of ~1.5 %). One pressure transducer (PCB®) was installed at a distance of 2.0 cm from the endwall and was coated with room-temperature vulcanizing (RTV) silicone to shield the transducer from heat effects. The pressure measured with this sensor was used as input for the data processing of the time-resolved CO measurements and for the chemical kinetics simulations. The setup is shown in Figure 1. Four sapphire windows were installed 2.0 cm upstream of the end wall at opposite sides of the shock tube for absorption and extinction measurements (Figure 1). The test mixtures were prepared manometrically in a 50-l stainless-steel mixing tank allowing to homogenize over night before use. Three mixtures were studied and are presented in table 1.

Table 1: Composition of the investigated mixtures. All mixtures contain 20 % He and are diluted in Ar.

Nr.	Mixture
Mix1	10 % CH_4 + 4.0 % O_2
Mix2	10 % CH_4 + 1 % DEE + 5.2 % O_2
Mix3	10 % CH_4 + 1 % CH_3OH + 4.3 % O_2

CO is used as a target species for the time-resolved temperature measurements based on two-color absorption in the infrared and He is added to accelerate vibrational relaxation of hot CO. A two-color fixed-wavelength absorption method was applied to determine time-resolved temperatures and CO concentrations. Figure 1 shows the schematics of the setup, for more details, see Ref. [7]. The wavelengths of two continuous-wave quantum-cascade lasers (QCL) were controlled by two QCL controllers (Arroyo instrument, QCL-6310) and were fixed at the center of two lines (v" = 0, P(8) and v" = 1, R(21) at 4.7359 and 4.5631 µm, respectively). The two laser beams were coupled into a single-mode fiber (InF3, Thorlabs) by an off-axis parabolic mirror. The two collinear beams are directed through the shock tube via two opposed sapphire windows. The transmitted beam is divided into two separate beams by a transparent quartz plate. Two bandpass filters (Spectrogon, NB-4560-135 nm and NB-4720-100 nm) in front of each detector (Vigo, PVI-3TE) were used for wavelength selection. A 25-cm absorption cell and a 20.25-m pathlength White cell filled with a gas mixture containing CO (1 %) were used to center the 4.7359-µm laser (AdTech Optics) and the 4.5631-µm laser (Hamamatsu), respectively.

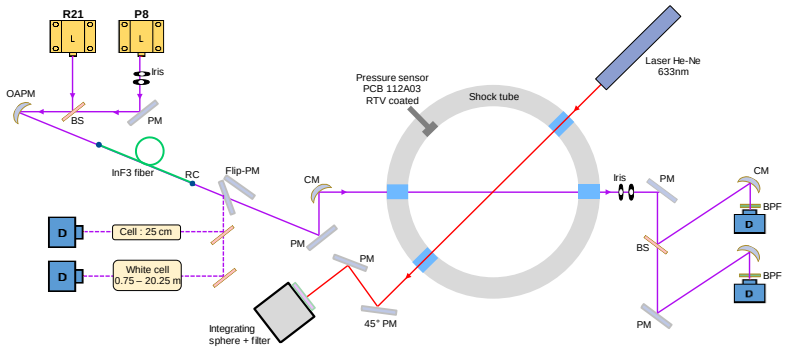

Figure 1: Schematics of the laser absorption (purple line) and the laser-extinction setup (red line). BS: beam splitter; BPF: bandpass filter; PM: planar mirror; OAPM: off-axis parabolic mirror; RC: reflective collimator; CM: concave mirror; D: detector.

Based on the Beer-Lambert law, the relationship between incident beam intensity and transmitted beam intensity can be expressed as $\left(I/I_0\right)_\nu = \exp\left(-pS(T)lx\varphi(\nu)\right)$, with p is the pressure, atm, $S(T)$ in $cm^{-2}bar^{-1}$ is the line strength at a certain temperature, l is the inner diameter of the shock tube and thus the absorption length, x is the species mole fraction, $\varphi(\nu)$ is the line shape that is assumed here to follow a Voigt function. The ratio $R(T)$ of the peak absorbance at the line center of both transitions is only a function of the temperature and the temperature can be calculated according to eq. 2:

$$T(R) = \left[\ln\frac{R(T)}{R(T_0)}\cdot\frac{k_B}{hc}\cdot\frac{1}{E_2'' - E_1''} + \frac{1}{T_0}\right]^{-1} \quad (2)$$

T_0 is the reference temperature (296 K), *E''* is the lower-state energy of the transition, h, c, k_B are the Planck constant, speed of light, and the Boltzmann constant, respectively. The line strengths of the P8 and R21 lines are taken from HITEMP database [14]. Collisional broadening coefficient and broadening index was taken from Ren et al. [7, 15]. Temperature and CO concentration profiles were calculated in an iterative way as described in our previous publications [7, 8].

Soot formation was observed by recording extinction of 633-nm radiation from a HeNe laser with an integrating sphere (Thorlabs, model IS236A-4) equipped with a 630±10-nm interference filter attached to a photodiode (model SM05PD1B) through side windows in the shock tube, 20 mm away from the end flange. The measurements were evaluated using the approach of the normalized optical densities D_{633nm} presented in [16]. The normalized optical density is given as $D_{633nm} = \ln(I_0/I)/[C]l$, with l is the absorption length, I_0 and I are the incident and transmitted signal respectively, and [C] is the total carbon concentration related to soot in the respective mixture.

Figure 2 presents typical temporal profiles of D_{633nm}. The optical density at a fixed time of 3.0 ms was chosen because the profiles reach the plateau value within the test time. This particular time was set according to the evolution of the pressure behind the reflected shock wave. Indeed, at a time of 3.0 ms, the cooling phase conditions were observed for all investigated mixtures (see pressure profile in Figure 2). Inception times τ were determined as the time between the pressure rise related to the arrival of the reflected shock wave from the fourth pressure transducer (20 mm away from the end flange) and the intersection of the tangent of the steepest rise in the HeNe laser signal to zero (Figure 2).

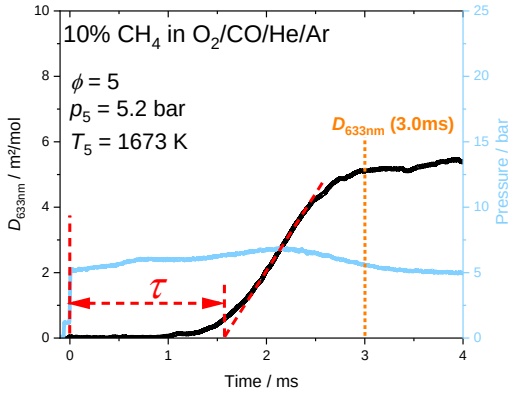

Figure 2: Pressure and temporal profiles of D_{633nm} and of the corresponding inception time τ.

3 Results and discussion

Figure 3 shows the measured temperature profiles during the oxidation of the investigated mixtures and also the predictions of three detailed kinetics mechanisms [9-11]. The simulation was performed with Chemical Workbench [17] using a "specified-pressure" reactor model with implementation of the measured pressure profile. For all mixtures, a temperature rises due to the oxidation of the fuel is observed before soot formation begins analogous to previous work [16]. The soot formation therefore proceeds at higher temperatures than T_5. Therefore, an accurate knowledge of the temperature profile during oxidation is necessary for soot modeling. For pure CH_4 (Figure 3a), good agreement between experiment and simulation is observed with the Aramco 3.0 mechanism [10] and the Fikri et al. [11] mechanism. Also, good agreement is observed with Yasunaga et al. mechanism [9] at higher temperatures (1706 and 1802 K). For CH_4/DEE (Figure 3b), no simulation was performed with Aramco 3.0 [10] since DEE is not included in this mechanism. A too slow prediction is noticed for both mechanisms (Fikri et al. [11] and Yasunaga et al. [9]) even if a better agreement is reached for the Yasunaga et al. [9] mechanisms at higher temperatures. Concerning the mixture with CH_3OH as additive (Figure 3c), the experiments were compared with the predictions of the Aramco3.0 mechanism and good agreement is observed in the whole temperature range.

The CO concentration profiles are also presented in Figure 3 together with the simulations with the aforementioned mechanisms. For pure CH_4 (Figure 3d), the best agreement is achieved with the Fikri et al. [11] and Aramco3.0 [10] mechanisms even if at the lowest temperature, the three tested mechanisms predict a too slow formation of CO. For CH_4/DEE (Figure 3e), the two tested mechanisms predict a too slow CO formation. When the plateau of CO formation is reached, the Yasunaga et al. [9] mechanism yields too high CO concentrations. This observation requires further analysis to understand the different shapes of experimental and simulated profiles. For CH_4/CH_3OH (Figure 3f), the simulation is slightly too fast but overall a good agreement is achieved similarly to the corresponding temperature measurements. Generally, slightly too high CO concentrations are predicted. The temperature and CO profiles show that methanol and especially diethyl ether leads to a faster ignition.

Figure 4a shows the optical density results. A characteristic "bell-shaped" curve as observed in the literature [3, 16] is found. For Mix1 (the reference mixture), the maximum optical density is reached at $T \approx 1700$ K with a value of $D_{633nm} \approx 5$ m^2/mol. DEE increases the soot yield slightly and lower soot yield is reached with CH_3OH compared to Mix1. The formation of soot is shifted towards lower temperature when using CH_3OH or DEE as additives. For instance, taking the CH_4 mixture at T = 1590 K as a reference, we notice that soot is formed at a temperature ~40 K lower for the mixture with CH_3OH as additive and at a temperature ~100 K lower for the mixture with DEE as additive. This can be explained by the faster ignition of the mixtures with additives.

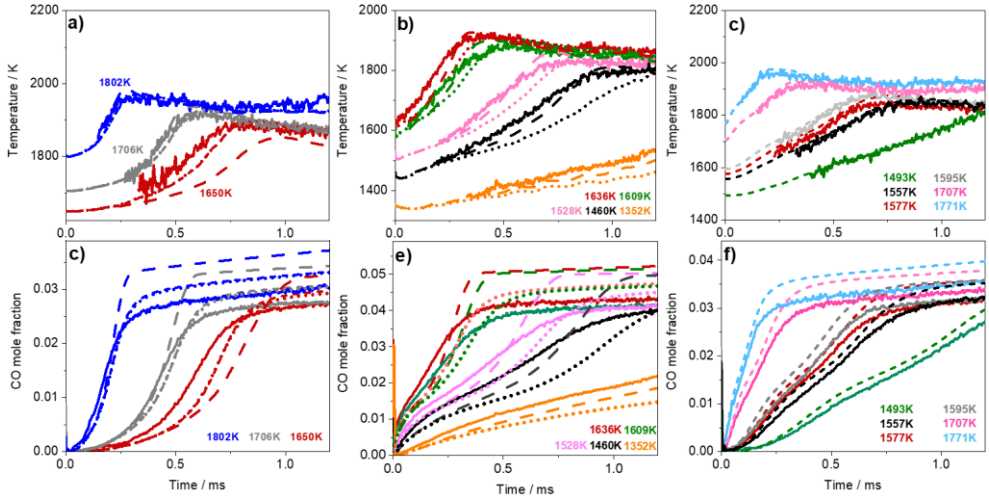

Figure 3: Top: Temperature profiles measured in different mixtures. Bottom: CO concentration profiles: a, d) Mix1; b, e) Mix2, and c, f) Mix3. All the experiments are compared with simulations based on the mechanisms of Yasunaga et al. [9] (dashed lines, frames a, b, d, e), Aramco 3.0 [10] (short dashed lines, frames a, c, d, f) and Fikri et al. [11] (short dotted lines, frames a, b, d, e).

Figure 4b presents the temperature dependence of the inception times of soot formation of the investigated mixtures. Longer inception times are observed for CH_4 and the shortest inception times were observed for DEE as additive. This behavior is attributed to the fact that the longest ignition delay times (IDTs) are observed for CH_4 and the shortest IDTs for CH_4/DEE [2].

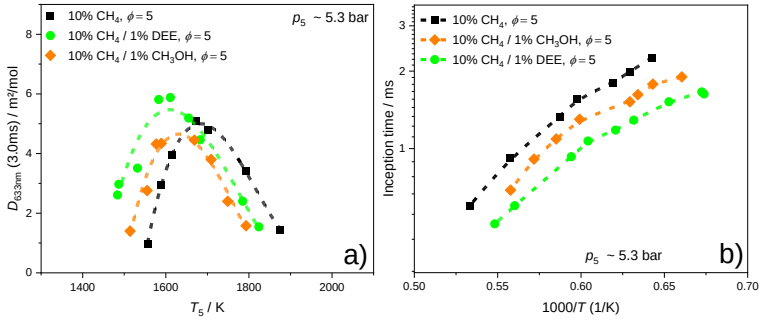

Figure 4: a) Optical density D_{633nm} measured at t = 3.0 ms in different mixtures. b) Temperature dependent inception times of soot formation for the studied mixtures.

4 Conclusions

The oxidation of fuel rich CH_4 mixtures (ϕ = 5) and the influence of two oxygenated additives (diethyl ether, methanol) on soot formation between 1484–1875 K at ~5 bar were studied in a shock tube. Temperature and CO concentrations were determined as a function of time after the arrival of the reflected shock wave using absorption measurements on the fundamental vibrational transitions of CO (P8 and R21). The experimental results were compared to the predictions of three detailed kinetics models (Yasunaga et al. [9], Aramco3.0 [10] and Fikri et al. [11]). Simulations with the Aramco3.0 mechanism showed very good agreement for the pure CH_4 and CH_4/CH_3OH experiments whereas the predictions from the mechanism of Yasunaga et al. agree quite well with the CH_4/DEE experiments. Laser-induced extinction experiments were also simultaneously performed. Soot yield and the corresponding inception times were measured. The major result of these experiments is that DEE increases the soot yield and that a slightly lower soot yield is reached with CH_3OH compared to pure

CH_4. The formation of soot is shifted towards lower temperature when using CH_3OH or DEE as additives. Other oxygenate additives will be tested whether they are better suited to prevent soot formation at very fuel-rich conditions in polygeneration processes and further kinetics analysis will be performed to understand the effect of these additives on the change in the initial routes of soot formation in future work.

5 Acknowledgements

Financial support by the German Research Foundation within the framework of the DFG research unit FOR 1993 “Multifunctional conversion of chemical species and energy” (Project number 229243862) is gratefully acknowledged.

References

[1] Atakan B, Kaiser SA, Herzler J, Porras S, Banke K, Deutschmann O, Kasper T, Fikri M, Schießl R, Schröder D, Rudolph C, Kaczmarek D, Gossler H, Drost S, Bykov V, Maas U, Schulz C. (2020). Flexible energy conversion and storage via high-temperature gas-phase reactions: The piston engine as a polygeneration reactor. Renew. Sust. Energ. Rev. 133: 110264.

[2] Herzler J, Sakai Y, Fikri M, Schulz C. (2019). Shock-tube study of the ignition and product formation of fuel-rich CH4/air and CH4/additive/air mixtures at high pressure. Proc. Combust. Inst. 37: 5705.

[3] Hong Z, Davidson DF, Vasu SS, Hanson RK. (2009). The effect of oxygenates on soot formation in rich heptane mixtures: A shock tube study. Fuel. 88: 1901.

[4] Zubel M, Heuser B, Pischinger S. (2017). 1-Octanol Tailor-made Fuel for Lower Soot Emissions. MTZ worldwide. 78: 58.

[5] Russo C, D'Anna A, Ciajolo A, Sirignano M. (2019). The effect of butanol isomers on the formation of carbon particulate matter in fuel-rich premixed ethylene flames. Combust. Flame. 199: 122.

[6] Sun K, Sur R, Chao X, Jeffries JB, Hanson RK, Pummill RJ, Whitty KJ. (2013). TDL absorption sensors for gas temperature and concentrations in a high-pressure entrained-flow coal gasifier. Proc. Comb. Inst. 34: 3593.

[7] He D, Nativel D, Herzler J, Jeffries JB, Fikri M, Schulz C. (2020). Laser-based CO concentration and temperature measurements in high-pressure shock-tube studies of n-heptane partial oxidation. Appl. Phys. B. 126: 142.

[8] He D, Shi L, Nativel D, Herzler J, Fikri M, Schulz C. (2020). CO-Concentration and Temperature Measurements in Reacting CH_4/O_2 Mixtures Doped with Diethyl Ether behind Reflected Shock Waves. Combust. Flame. 216: 194.

[9] Yasunaga K, Simmie JM, Curran HJ, Koike T, Takahashi O, Kuraguchi Y, Hidaka Y. (2011). Detailed chemical kinetic mechanisms of ethyl methyl, methyl tert-butyl and ethyl tert-butyl ethers: The importance of uni-molecular elimination reactions. Combust. Flame. 158: 1032.

[10] Zhou C-W, Li Y, Burke U, Banyon C, Somers KP, Ding S, Khan S, Hargis JW, Sikes T, Mathieu O, Petersen EL, AlAbbad M, Farooq A, Pan Y, Zhang Y, Huang Z, Lopez J, Loparo Z, Vasu SS, Curran HJ. (2018). An experimental and chemical kinetic modeling study of 1,3-butadiene combustion: Ignition delay time and laminar flame speed measurements. Combust. Flame. 197: 423.

[11] Fikri M, Sakai Y, Herzler J, Schulz C. (2017). Experimental and numerical study of the ignition delay times of primary reference fuels containing diethylether. Proceedings of the 26th International Colloquium on the Dynamics of Explosions and Reactive Systems. Paper Nr. 957.

[12] Fikri M, Makeich A, Rollmann G, Schulz C, Entel P. (2008). Thermal Decomposition of Trimethylgallium $Ga(CH_3)_3$: A Shock-Tube Study and First-Principles Calculations. J. Phys. Chem. A. 112: 6330.

[13] Nativel D, Cooper SP, Lipkowicz T, Fikri M, Petersen EL, Schulz C. (2020). Impact of shock-tube facility-dependent effects on incident- and reflected-shock conditions over a wide range of pressures and Mach numbers. Combust. Flame. 217: 200.

[14] Rothman LS, Gordon IE, Barber RJ, Dothe H, Gamache RR, Goldman A, Perevalov VI, Tashkun SA, Tennyson J. (2010). HITEMP, the high-temperature molecular spectroscopic database. J. Quant. Spectrosc. Ra. 111: 2139.

[15] Ren W, Farooq A, Davidson DF, Hanson RK. (2012). CO concentration and temperature sensor for combustion gases using quantum-cascade laser absorption near 4.7 μm. Appl. Phys. B. 107: 849.

[16] Drakon A, Eremin A, Mikheyeva E, Shu B, Fikri M, Schulz C. (2018). Soot formation in shock-wave-induced pyrolysis of acetylene and benzene with H_2, O_2, and CH_4 addition. Combust. Flame. 198: 158.

[17] Deminsky M, Chorkov V, Belov G, Cheshigin I, Knizhnik A, Shulakova E, Shulakov M, Iskandarova I, Alexandrov V, Petrusev A, Kirillov I, Strelkova M, Umanski S, Potapkin B. (2003). Chemical Workbench—integrated environment for materials science. Comp. Mater. Sci. 28: 169.